

# Polymer Crystallization and Precipitation-Induced Wrapping of Carbon Nanofibers with PBT

Gaurav Mago,<sup>1</sup> Dilhan M. Kalyon,<sup>2</sup> Frank T. Fisher<sup>1</sup>

<sup>1</sup>Department of Mechanical Engineering, Stevens Institute of Technology, Hoboken, New Jersey 07030

<sup>2</sup>Highly Filled Materials Institute and Department of Chemical Engineering and Materials Science, Stevens Institute of Technology, Hoboken, New Jersey 07030

Received 1 February 2009; accepted 5 April 2009

DOI 10.1002/app.30623

Published online 18 June 2009 in Wiley InterScience (www.interscience.wiley.com).

**ABSTRACT:** Carbon nanofibers (CNFs) have attracted significant interest because of their excellent mechanical, electrical, and physical properties. Recent advances in chemical functionalization strategies are anticipated to extend their utility in various applications. In this study, noncovalent methods of CNF functionalization utilizing solution crystallization and precipitation techniques were used to create hybrid nanostructures consisting of CNFs and poly(butylene terephthalate) (PBT). Key to this study is the finding that *o*-chlorophenol can be used as a suitable solvent to dissolve PBT to generate these nanostructures. PBT crystallization was documented via wide-angle X-ray analysis and differential scanning calorimetry

and was due to the nucleation effect of the CNFs. The sizes of the PBT crystals could be manipulated by altering the polymer concentration. The solution crystallization and precipitation techniques provide an alternative strategy to alter and control the nanostructure/polymer interface. The resulting nanohybrid structures may potentially find use in a broad range of applications including electronic devices, sensors, and as reinforcing agents in a polymer matrix. © 2009 Wiley Periodicals, Inc. *J Appl Polym Sci* 114: 1312–1319, 2009

**Key words:** hybrid nanostructures; carbon nanofiber; nanocomposites; crystallization; precipitation

## INTRODUCTION

Poly (butylene terephthalate) (PBT) is a semicrystalline engineering thermoplastic polymer with relatively high melting temperature, low glass transition temperature, and fast crystallization rate and is easily shaped using conventional molding methodologies. It is widely utilized in applications ranging from electronics and telecommunication equipment to the automotive industry in both “under the hood” and exterior applications.<sup>1</sup> PBT is thus an excellent candidate for use in various nanocomposite applications involving carbon nanofibers (CNFs), in which CNFs are of interest because of their excellent mechanical, electrical, and physical properties that they can impart to polymer systems.<sup>2–8</sup>

Generally, the gains in ultimate physical properties for polymer nanocomposites depend on the state of dispersion of the nanoparticles within the polymeric matrix and the interfacial interactions between the polymer and nanoparticles.<sup>9–13</sup> To control the interfacial properties between the polymeric matrix and the nanoparticles, various functionalization techniques have been developed, such as covalent<sup>14–16</sup>

and noncovalent functionalization methods.<sup>17</sup> Covalent functionalization strategies typically include an oxidation step where defects are intentionally introduced within the structure to enable sites for further covalent chemistry. The physical properties of the individual carbon nanostructures, including electrical and mechanical properties, have been observed to decrease as a result of covalent functionalization due to the introduction of these defect sites.<sup>18</sup> Such deterioration of properties are not anticipated when noncovalent functionalization methods including solution crystallization, precipitation, and physical vapor deposition are applied.<sup>17–20</sup> Reports of noncovalent functionalization methods used to create hybrid nanostructures of carbon nanotubes (CNTs) with polyethylene (PE),<sup>21,22</sup> nylon-6,6,<sup>23</sup> and poly(ethylene glycol) (PEG)<sup>24</sup> have been reported in the literature.

For the solution crystallization technique, the polymer is crystallized from its solution and the crystals grow epitaxially on the surfaces of the CNTs, generally leading to the formation of nanohybrid shish-kebab (NHSKs) structures consisting of a long nanotube in the core (shish) with crystals grown on its surface as kebab.<sup>21</sup> For example, Haggenueller et al.<sup>25</sup> used a hot-coagulation technique to crystallize PE in the presence of CNTs to generate a NHSK microstructure, with their results suggesting that

Correspondence to: F. T. Fisher (frank.fisher@stevens.edu).

this method can be used to produce polymer nanocomposites containing a high loading of nanotubes with the possibility of controlling the nanotube-polymer interface. In another study with poly(vinyl alcohol) (PVA), it was found that nanotubes coated with crystalline PVA resulted in significant improvements in nanocomposite mechanical properties.<sup>26</sup>

On the other hand, in the precipitation technique, an antisolvent is used to induce rapid phase separation and crystallization of the polymer from solution. Precipitation techniques involving suitable solvent/antisolvent combinations have been used to grow polymer crystals on the surface of multiwalled carbon nanotubes (MWNTs) in conjunction with PE,<sup>22,27</sup> PVA and PEG,<sup>24</sup> fluorinated graft polymers,<sup>28</sup> PVDF,<sup>29</sup> and amorphous polymers like PMMA.<sup>30</sup> Coprecipitation techniques were also applied to modify the surfaces of CNTs with polyhydroxyamide (PHA).<sup>31</sup> With PVDF, it was reported that certain combinations of antisolvent and nanofillers give rise to the formation of the piezoelectric  $\beta$ -crystal structures in PVDF nanocomposites,<sup>4</sup> whereas the  $\alpha$ -polymorph of PVDF is preferentially formed in conventional processing techniques.<sup>32</sup>

To date, such solution crystallization and precipitation methods for the noncovalent functionalization of carbon nanostructures with PBT have not been reported in the literature, likely due to the difficulties associated with the solubilization of PBT in conventional solvents. Here, the successful creation of hybrid CNF-PBT nanostructures is reported for both solution crystallization and precipitation based noncovalent techniques using the solvent *o*-chlorophenol. The effects of the processing conditions on the microstructure development of the PBT nanocomposites are also investigated. The resulting nanohybrid structures coated with PBT could find potential use in a broad range of industrial applications, including electronic devices, sensors, and as reinforcing agents in a polymer matrix.<sup>17,18,33</sup>

## EXPERIMENTAL

### Materials

PBT pellets were obtained from Ticona Polymers (Shelby, NC). Vapor-grown CNFs were obtained from Applied Science (Cedarville, OH) (trade name: Pyrograf-III). The diameters of the CNFs were in the 60–150 nm range (mean diameter of 70 nm). The lengths of the CNFs were in the 30–100  $\mu\text{m}$  range. Figure 1 shows a typical scanning electron micrograph (SEM) of the as-received CNFs. The mean bulk density of the as-received CNFs was 1.95 g/cm<sup>3</sup>. After an extensive solubility study of PBT, *o*-chlorophenol (GC grade >98%), and acetone (HPLC grade >99.9%) were purchased from Sigma-Aldrich

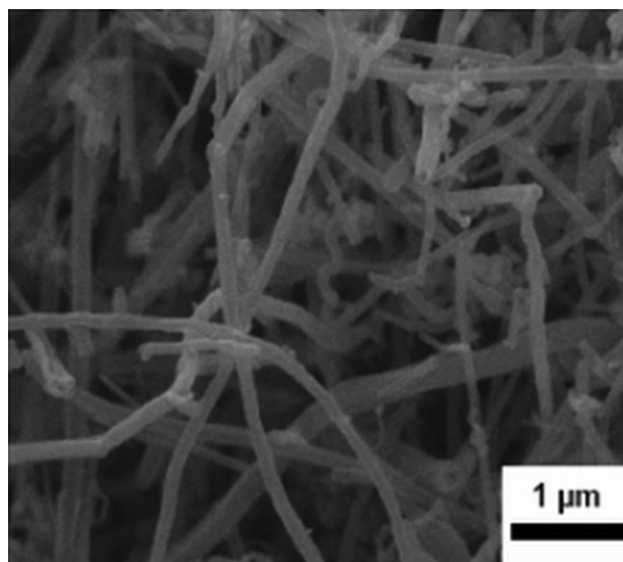


**Figure 1** Scanning electron micrograph of the as-received carbon nanofibers.

(St. Louis, MO) and selected as the solvent and antisolvent, respectively.

As discussed later, both the solution crystallization and precipitation techniques were applied as means to coat the CNFs with PBT crystals. Imaging using polarized light microscopy and SEM, as well as differential scanning calorimetry (DSC) and wide-angle X-ray diffraction analysis (WAXD) techniques, was utilized to characterize the crystallization behavior and the crystal morphology of the resulting hybrid CNF-PBT nanostructures.

### Solution crystallization of PBT and CNF-PBT samples

An initial polymer solution (2 wt %) was prepared by dissolving the PBT pellets in *o*-chlorophenol at 150–160°C for 2 h. A suspension of *o*-chlorophenol and 0.1 wt % CNF was prepared by ultrasonication for 1 h at room temperature using a Misonix XL-2020 sonicator (100–120 W, amplitude 5). Equal parts of the 0.1% CNF suspension and 2% PBT solution were then mixed at 150–160°C under continuous magnetic stirring for 1 h. The resulting mixture was slowly cooled down to 30–40°C, after which a few drops of the mixture were placed between glass slides and maintained at this temperature for 24 h. The formed crystals were analyzed under polarized light using a Nikon OPTIPHOT-POL2 optical microscope. To further understand the morphology, the crystallized CNF-PBT solution (prepared by mixing equal parts of 0.1% CNF suspension and 2% PBT solution in *o*-chlorophenol) was filtered and washed repeatedly with methanol, followed by overnight drying in vacuum oven at 50°C. The dried samples were gold coated and analyzed under SEM (LEO

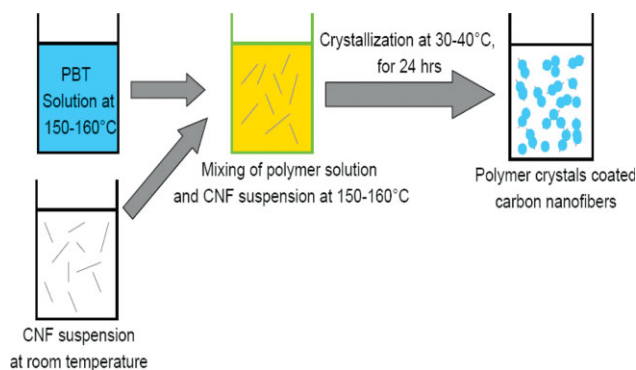


**Figure 2** Solution crystallization of PBT in the presence of carbon nanofibers. [Color figure can be viewed in the online issue, which is available at [www.interscience.wiley.com](http://www.interscience.wiley.com).]

1550) at 10 kV. Figure 2 shows the procedure used to prepare the PBT-coated CNFs using solution crystallization technique. Pure PBT crystallized under identical conditions was used as a control. The effect of polymer concentration on the crystal size was studied by preparing PBT solutions with differing concentrations of PBT under similar conditions.

#### Precipitation of PBT and CNF-PBT samples

For the precipitation technique, a PBT solution (2 wt %) was again prepared by dissolving the PBT pellets in *o*-chlorophenol at 150–160°C for 2 h. A suspension of *o*-chlorophenol with 0.1 wt % CNF was prepared by ultrasonication at room temperature for 1 h using the Misonix XL-2020 sonicator (100–120 W, amplitude 5) and then mixed with the PBT solution (equal parts) at 150–160°C, with continuous stirring for 1 h. As shown in Figure 3, the mixture was slowly cooled down to 65–75°C, after which the antisolvent acetone was added (at an antisolvent over the mixture weight ratio of 2.5). This resulted in the formation of gray-colored CNF-PBT precipitate. The CNF-PBT precipitate contained approximately 4.8 wt % of CNFs. The precipitate was filtered and washed with acetone to completely remove the *o*-chlorophenol solvent. Samples of pure PBT precipitate were also prepared using the same solvent/antisolvent method. Precipitate samples were dried in a vacuum oven for 24 h at 50°C followed by SEM microstructural analysis using a LEO 1550 SEM at 10 kV. The samples were sputter coated with gold before SEM analysis.

#### Thermal analysis and WAXD analysis

To understand the effects of CNFs on the crystallinity and crystallization behavior of the CNF-PBT precipitates, DSC studies were conducted using a TA Instruments (New Castle, DE) DSC model Q100. The DSC samples were heated and cooled between 25

and 250°C at constant heating and cooling rates of 10°C/min (the samples were maintained under isothermal conditions at 25 and 250°C for 5 min before temperature ramping). The onset of melting ( $T_{m,o}$ ) and nominal peak melting ( $T_{m,p}$ ) temperatures were obtained during heating of PBT from 25 to 250°C. The melting temperature ( $T_m$ ) of PBT is defined as the highest temperature at which the last trace of crystallinity is revealed upon heating. The onset of crystallization ( $T_{c,o}$ ) and nominal crystallization ( $T_{c,p}$ ) temperatures were obtained during cooling from 250°C to 25°C.

The relative degree of crystallinity was determined as the ratio of the integrated heat of fusion of the sample over the heat of fusion of purely crystalline PBT, i.e., 140 J/g.<sup>34</sup> WAXD analysis was also performed by placing the samples on a quartz sample holder using a Rigaku Miniflex diffractometer in conjunction with a Cu  $K_\alpha$  radiation source ( $\lambda = 0.154$  nm) operated at 30 kV. In addition, samples of the PBT precipitates and as-received PBT were compression molded using a Carver hot press at 245°C for 5 min to enable comparison and further WAXD analysis.

## RESULTS AND DISCUSSION

#### Solution crystallization of PBT and CNF-PBT nanocomposites

Figure 4 shows the typical polarized light micrographs of the solution-crystallized pure PBT samples with 2% and 5% (by weight) PBT concentrations after 24 h. Upon cooling of the solution of PBT in *o*-chlorophenol, PBT forms birefringent spherulites. Figure 4 also shows that there is an increase of the PBT spherulite size from about 10–15  $\mu\text{m}$  to approximately 70  $\mu\text{m}$  as the PBT concentration increased from 2 to 5 wt %. This increase of the spherulite size is expected on the basis of the greater availability of PBT at higher concentrations.<sup>35</sup> Because the *o*-chlorophenol solvent has a boiling temperature around

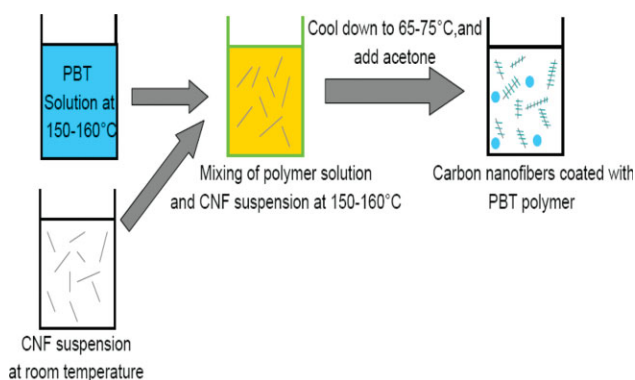


**Figure 3** Solution precipitation of PBT in the presence of carbon nanofibers. [Color figure can be viewed in the online issue, which is available at [www.interscience.wiley.com](http://www.interscience.wiley.com).]

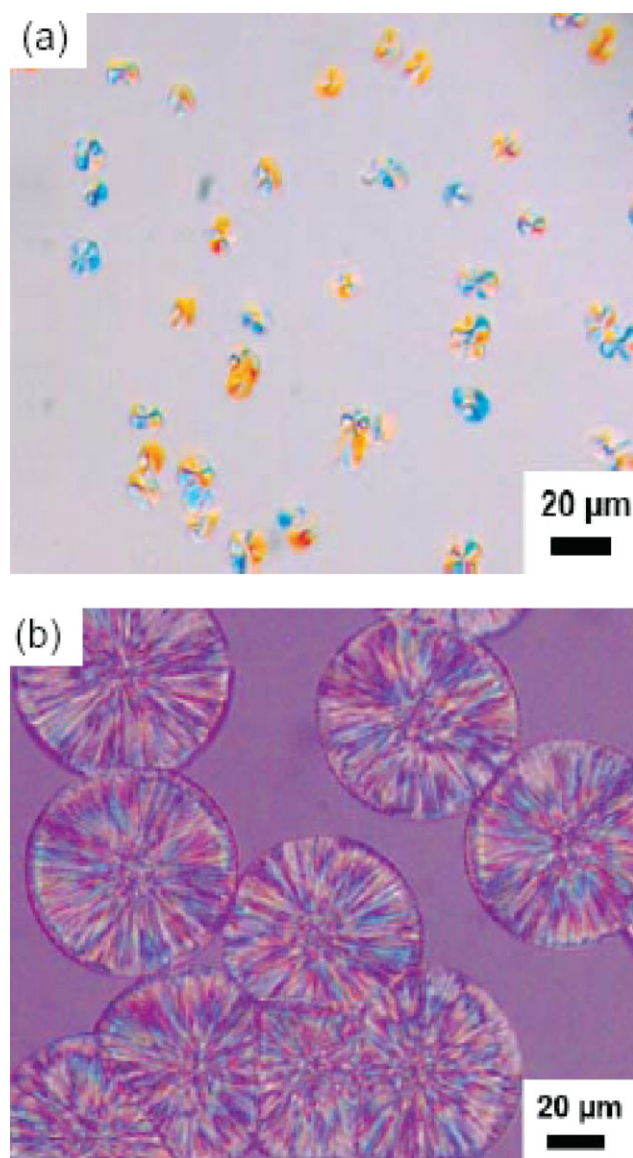


**Figure 4** Polarized light optical micrographs of crystallized solutions: (a) 2% PBT solution and (b) 5% PBT solution. Each sample was allowed to crystallize for 24 h. [Color figure can be viewed in the online issue, which is available at [www.interscience.wiley.com](http://www.interscience.wiley.com).]

175°C, the evaporation of the solvent in this processing method is minimal and a two-phase system is developed, consistent with the PBT in epoxy study of Nichols and Robertson,<sup>36,37</sup> in which they found that at relatively high temperatures, the PBT/epoxy system consists of a single-phase liquid (clear solution), but that as the temperature is decreased to below 155°C, phase separation occurs to give rise to PBT spherulites of uniform size. In their work, the average spherulite size was 35 μm.

Figure 5 shows typical polarized light micrographs of PBT solution containing CNFs at two different magnifications. PBT crystals with the characteristic Maltese cross patterned structures

grown on the surfaces of the CNFs can be clearly observed, with decrease of the PBT crystal sizes presumably occurring due to the heterogeneous nucleation effect (higher nucleation rates give rise to greater number of crystallites). Some crystals of what appears to be pure PBT can also be identified in the solution, indicating that the crystallization would also occur in the absence of the nanofibers. In other works, the polymer concentration and crystallization conditions were shown to affect the morphology generated upon solution crystallization, with a low crystallization temperature favoring homogeneous nucleation

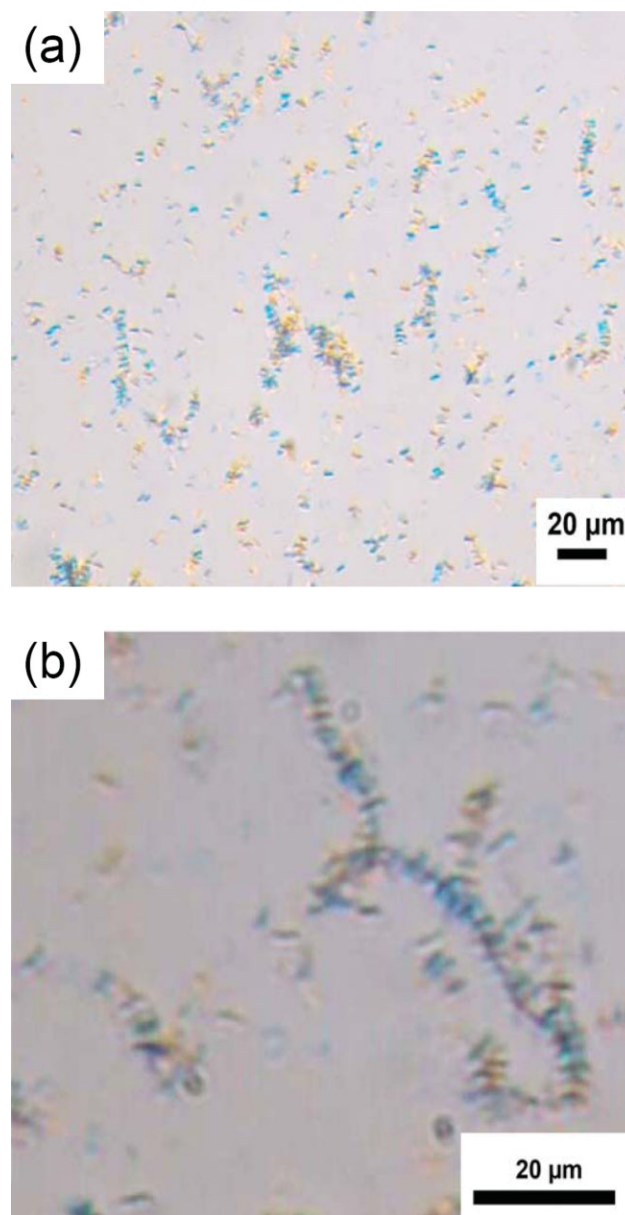


**Figure 5** Solution crystallization of PBT on carbon nanofibers: (a) low magnification image and (b) high magnification image taken at different locations (crystallization time of 24 h). [Color figure can be viewed in the online issue, which is available at [www.interscience.wiley.com](http://www.interscience.wiley.com).]

and high temperature favoring heterogeneous nucleation.<sup>38</sup>

For a detailed understanding of the growth of polymer crystals on the surface of CNFs, SEM analysis was performed on the crystallized samples. Figure 6 shows the SEM micrograph of PBT crystallized on the surface of CNFs (prepared using solution crystallization). The prominent PBT single crystals can be seen to have grown perpendicularly on the surface of CNFs, and the CNFs cannot be seen directly. These structures have been suggested as “overgrown NHSKs” by Kodjie et al.<sup>39</sup> They obtained similar overgrown NHSKs during solution crystallization of HDPE in the presence of single-walled CNTs and suggested that the unique orientation of the polymer lamellae on the surface of nanotubes can lead to an “open” morphology. The SEM results obtained for PBT in the presence of CNFs, along with the results obtained with polarized microscopy, confirm that the solution crystallization technique can be used to coat/wrap nanoparticles with PBT.

Earlier work has also demonstrated that micron-sized glass fibers can also act as nucleating agents during solution crystallization of a 5% PBT solution in hexafluoroisopropanol (HFIP).<sup>40</sup> The crystal sizes of PBT were observed to decrease because of the incorporation of glass fibers into the polymer solution. Park et al.<sup>41</sup> have also studied the crystallization kinetics as well as nucleation effects of high loadings of glass fibers (30 wt %, 10  $\mu\text{m}$  diameter, approximately 300  $\mu\text{m}$  in length) in PBT dissolved in 10% TFA- $\text{CCl}_4$  (10% trifluoro acetic acid-carbon tetrachloride solution) and found that the filler particles led to an increase of the rate of crystallization. Such heterogeneous nucleation effects have also been noted to occur on nanofiller surfaces during melt as well as solution crystallization of other semicrystalline polymers including PE, nylon-6,6, poly(propylene) (PP), and poly(ethylene naphthalate) (PEN).<sup>21,42–45</sup> A decrease in polymer crystal size and an increase in the rate of crystallization have also been observed during various studies performed under shear as well as under quiescent conditions.<sup>43,44,46</sup>

#### Precipitation of PBT and CNF-PBT nanostructures

Representative SEM micrographs of the 4.8% CNF-PBT precipitates obtained upon the solvent–antisolvent precipitation process are shown in Figure 7. The polymer precipitation takes place due to the interdiffusion of solvent and antisolvent, with the rate of interdiffusion dependent on the solubility parameters of the solvent and antisolvent used.<sup>47–49</sup> It has previously been shown that the precipitate morphology depends on the type of solvent, antisolvent, and the presence of nanoparticles.<sup>4</sup> Figure 7(a)

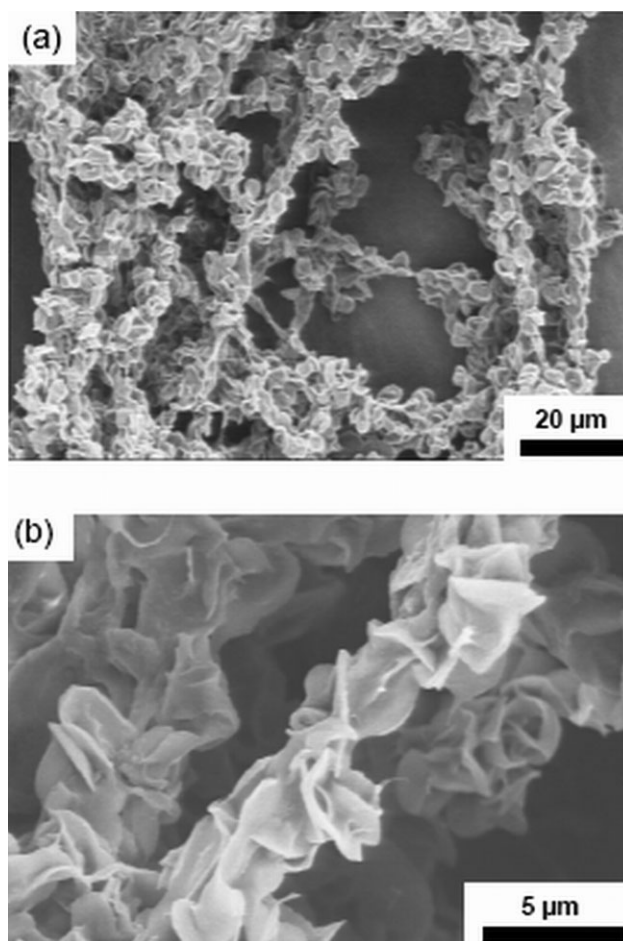


**Figure 6** SEM micrographs of PBT solution crystallized on carbon nanofibers: (a) low magnification image and (b) high magnification image taken at a different location (crystallization time of 24 h).

shows a SEM micrograph (taken at low magnification) of the PBT-coated CNF precipitate. It can be seen that all CNFs are uniformly coated with PBT, indicating that the heterogeneous nucleation effect is the dominant crystallization mechanism under the processing conditions shown in Figure 3 (see also the next section). It should be noted that small PBT crystals also formed upon the addition of the acetone antisolvent into the PBT suspension containing CNFs (not shown). This is due to the rapid rate of polymer precipitation and partial nucleation/growth of the polymer away from the CNF surface, as was also observed by Zhang et al.<sup>24</sup> during precipitation of PEG in the presence of CNTs (using supercritical carbon dioxide as the antisolvent). Li et al.<sup>23</sup> obtained similar heterostructures (CNF in core and polymer crystals grown on its surface) during solution crystallization of nylon-6,6 in the presence of CNFs. Similar structures have been obtained during precipitation of approximately 1.5 wt % PHA solution containing around 30 wt % MWNTs when water was used as an antisolvent. In that work it

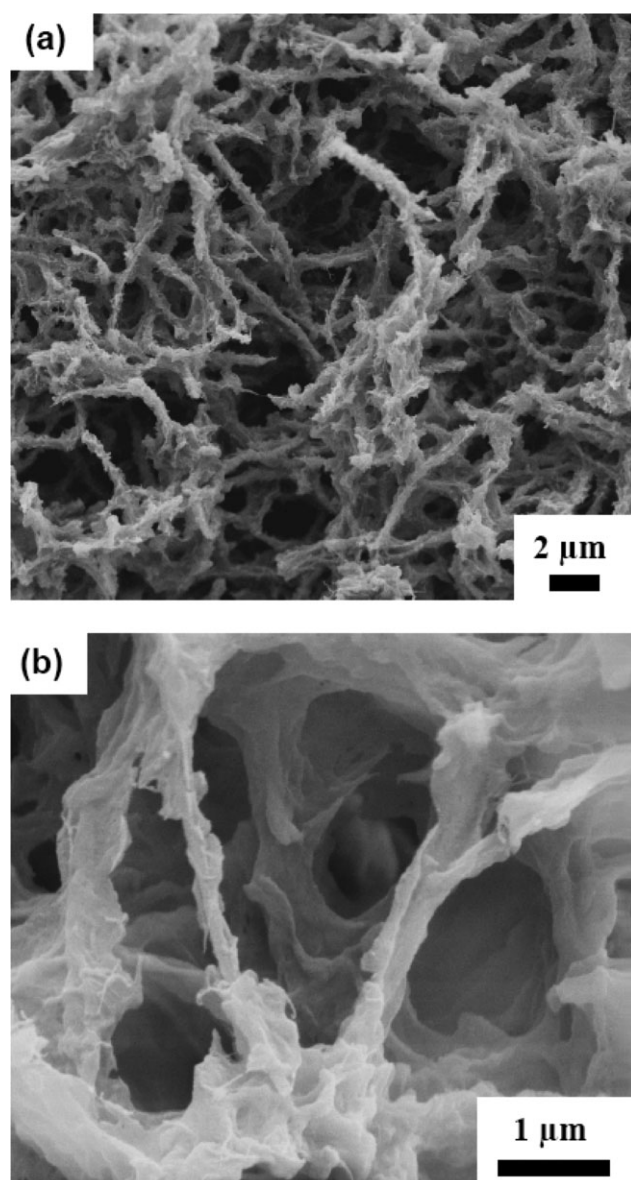


**Figure 7** SEM images of PBT-coated CNFs prepared via precipitation technique: (a) low magnification image and (b) high magnification image.

was observed that the presence of PHA layer on the surface of MWNTs increases the solubility of the nanotubes in polar solvents.<sup>31</sup>

#### Thermal analysis of PBT and PBT coated CNFs prepared using the precipitation technique

The impact of CNFs on the crystallization behavior and crystallinity of 4.8% CNF-PBT precipitate was studied using DSC under quiescent conditions. Figure 8 shows DSC scans of as-received PBT, PBT precipitates, melt-pressed PBT precipitates, and 4.8% CNF-PBT precipitates at a heating and cooling rate of 10°C/min. The melting onset temperature ( $T_{m,o}$ ), nominal melting temperature ( $T_{m,p}$ ), crystallization onset temperature ( $T_{c,o}$ ), nominal crystallization tem-

perature ( $T_{c,p}$ ), and degree of crystallinity ( $X_c$ ) of as-received PBT, PBT precipitates, CNF-PBT precipitates, and melt-pressed PBT precipitates are given in Table I. Table I shows that a decrease of the onset of melting temperature ( $T_{m,o}$ ) occurs in PBT and 4.8% CNF-PBT precipitates in comparison with those of the as-received PBT and melt-pressed PBT precipitates, respectively. The decreases in the onset of the melting temperature  $T_{m,o}$  could be associated with the formation of crystalline defects or small size of crystals during precipitation as observed with the WAXD analysis of these samples (as discussed further in the next section).<sup>50,51</sup>

In crystalline polymers, the factors contributing to the reduced melting temperature arise from the finite size of the crystallites, their state of internal perfection, and the interfacial and connecting regions.<sup>52</sup> Since crystallization is conducted at finite rates, the deviations from equilibrium that result manifest themselves in reduced thermodynamic stability and lower melting temperature of the crystallites formed.<sup>50,52</sup> On the other hand, no significant changes were observed in the nominal melting temperature  $T_{m,p}$  and the melting temperature  $T_m$  of the samples shown in Table I.

Higher crystallinity ( $X_c$ ) values were observed in the 4.8% CNF-PBT precipitates in comparison with those of the pure PBT precipitate samples (see Table I). The increased crystallinity can be attributed to the high surface area and the associated heterogeneous nucleation effect of the CNFs. An increase in crystallinity upon the addition of MWNTs has likewise been observed for other polymers such as PVA<sup>53</sup> and PVDF,<sup>44</sup> whereas a decrease in crystallinity has been observed for poly(ethylene oxide) (PEO) nanocomposites.<sup>54</sup> It appears that the incorporation of the CNTs or nanofibers can either promote or hinder the

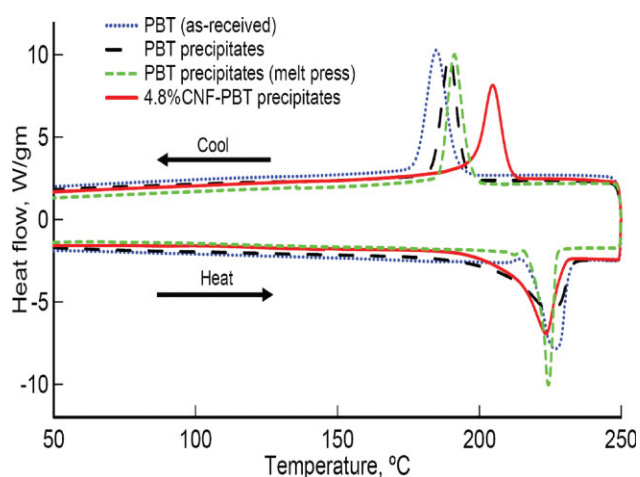


**Figure 8** Typical DSC scans for different samples during heating and cooling at 10°C/min. [Color figure can be viewed in the online issue, which is available at [www.interscience.wiley.com](http://www.interscience.wiley.com).]

**TABLE I**  
**Thermal Analysis of PBT and 4.8% CNF-PBT Precipitates Prepared via Precipitation Technique and Comparison of Melt-Pressed Pure PBT and PBT Precipitate Samples**

Sample	$T_{m,o}$ (°C)	$T_{m,p}$ (°C)	$T_m$ (°C)	$X_c$ (%)	$T_{c,o}$ (°C)	$T_{c,p}$ (°C)
As-received PBT	216	227.2	235.2	20.0	197.5	184.8
PBT precipitate	186.9	225	235.5	28.1	199.9	189.5
4.8% CNF-PBT precipitate	188.3	223.5	232.8	32.2	215.6	204.7
PBT precipitate (melt pressed)	215.3	224.4	229.5	21.4	201.9	191.2

crystallization process, presumably affected by a number of factors including the molecular weight and short and long chain branch distributions of the macromolecules that can alter crystallinity development within the nanocomposite.

An increase in crystallinity in PBT precipitates (when compared with the as-received PBT and melt-pressed PBT precipitates) highlights the important role that the processing history plays on the development of the crystalline morphology of the precipitated PBT.<sup>55,56</sup> Furthermore, it has been observed that changes in crystallinity can significantly affect various physical properties of the processed polymer sample.<sup>57,58</sup> In addition, because of the heterogeneous nucleation effect in the presence of CNFs, there is an increase in nominal crystallization temperature ( $T_{c,p}$ ) as well as onset crystallization temperature ( $T_{c,o}$ ) of 4.8% CNF-PBT precipitates in comparison with pure PBT precipitates processed under similar conditions. An increase in the crystallization temperature of melt-pressed PBT precipitates in comparison with that of as-received PBT might be due to an increase in the nucleation rate as suggested by other studies focusing on the effects of the precipitation technique on the crystallization behavior of semicrystalline polymers.<sup>59,60</sup>

### WAXD analysis of PBT and CNF-PBT precipitates prepared using the precipitation technique

Figure 9 shows the WAXD patterns of as-received PBT, PBT precipitate, 4.8% CNF-PBT precipitate, and melt-pressed pure PBT precipitate samples. Generally, it has been found that the major peaks of PBT appear at  $2\theta$  angles of 15.8°, 17.0°, 20.5°, 23.2°, 25.0°, 29.3°, and 31.2°.<sup>61,62</sup> It can be seen that for the PBT and 4.8% CNF-PBT precipitate samples, the peaks at 15.8° and 17.0° have merged together, with an increase in intensity for the precipitate samples. The broadening of the peaks in the WAXD spectrum can be associated with the reduction of the crystalline order, i.e., an increase of crystalline defects or the reduction of the crystallite sizes.<sup>52</sup> Thus, both the DSC and WAXD results suggest the introductions of imperfections/defects into the crystalline morphologies and/or the formation of relatively small crystals upon the precipitation process. Similarly, for these samples, the peaks at 23.2° and 25° are broad and appear to be merged together. On the other hand, sharper peaks at  $2\theta$  angle of 15.8°, 17.0°, 20.5°, 23.2°, and 25.0° can be seen for the as-received PBT and melt-pressed PBT precipitate samples, suggesting enhanced crystalline order or increase of the crystal size in comparison with the precipitated PBT samples. Thus, the melt-pressing method can be used to reverse the effects of precipitation for the pure PBT samples.

### CONCLUSIONS

This work reports the first demonstration of CNFs successfully coated with crystals of the semicrystalline engineering thermoplastic PBT using both solution crystallization and precipitation techniques. An initial solubility study found *o*-chlorophenol to be a suitable solvent for PBT. NHSK-type CNF-PBT hybrid nanostructures were observed upon the application of the solution crystallization and precipitation methods. The crystal size depends on the concentration of the polymer in the solution. The heterogeneous nucleation mechanism appears to play an important role in the creation of these hybrid nanostructures, and one must carefully select the crystallization conditions such that heterogeneous crystallization is the dominant crystallization mechanism. DSC results indicate a decrease of the

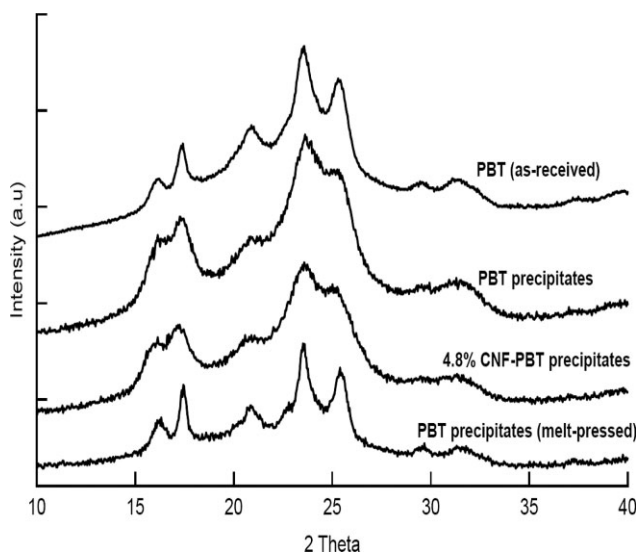


**Figure 9** WAXD samples of as-received PBT, PBT precipitates, 4.8% CNF-PBT precipitates, and melt-pressed PBT precipitates.

temperature at which the onset of melting occurs, and WAXD results show a broadening of the peaks associated with PBT crystallinity in the WAXD spectrum. These results suggest the introduction of crystalline imperfections/defects or reductions in crystallite sizes upon the relatively fast crystallization conditions experienced by PBT during the precipitation process.

The authors thank Dr. Halil Gevgilili from the Highly Filled Materials Institute (HfMI) at Stevens for his contributions to this work. They also thank Dr. Stephen Bartolucci (US Army Benet Laboratories, Watervliet Arsenal, NY) for providing the CNFs.

## References

- Gallucci, R. R.; Patel, B. R. *Poly(butylene terephthalate)*; Wiley: Chichester, England, 2003; p 293.
- Vigolo, B.; Penicaud, A.; Coulon, C.; Sauder, C.; Pailler, R.; Journet, C.; Bernier, P.; Poulin, P. *Science* 2000, 290, 1331.
- Shah, D.; Maiti, P.; Gunn, E.; Schmidt, D. F.; Jiang, D. D.; Batt, C. A.; Giannelis, E. P. *Adv Mater* 2004, 16, 1173.
- Mago, G.; Kalyon, D. M.; Fisher, F. T. *J Nanomater* 2008, 3, 759825.
- Kharchenko, S. B.; Douglas, J. F.; Obrzut, J.; Grulke, E. A.; Migler, K. B. *Nat Mater* 2004, 3, 564.
- Liu, T.; Phang, I. Y.; Shen, L.; Chow, S. Y.; Zhang, W. *Macromolecules* 2004, 37, 7214.
- Pasquali, M. *Nat Mater* 2004, 3, 509.
- Demirkol, E.; Kalyon, D. M. *J Appl Polym Sci* 2007, 104, 1391.
- Coleman, J. N.; Khan, U.; Gun'ko, Y. K. *Adv Mater* 2006, 18, 689.
- Strano, M. S. *Nat Mater* 2006, 5, 433.
- Coleman, J. N.; Khan, U.; Blau, W. J.; Gun'ko, Y. K. *Carbon* 2006, 44, 1624.
- Moniruzzaman, M.; Winey, K. I. *Macromolecules* 2006, 39, 5194.
- Zhang, W.; Picu, R. C.; Koratkar, N. *Nanotechnology* 2008, 19, 285709.
- Hirsch, A. *Angew Chem Int Ed* 2002, 41, 1853.
- Hirsch, A.; Vostrowsky, O. In *Topics in Current Chemistry*; Schlüter, A.D., Ed., 2005; Vol. 245, p 193.
- Balasubramanian, K.; Burghard, M. *Small* 2005, 1, 180.
- Baskaran, D.; Mays, J. W.; Bratcher, M. S. *Chem Mater* 2005, 17, 3389.
- Star, A.; Stoddart, J. F.; Steuerman, D.; Diehl, M.; Boukai, A.; Wong, E. W.; Yang, X.; Chung, S. W.; Choi, H.; Heath, J. R. *Angew Chem Int Ed* 2001, 40, 1721.
- Liu, L.; Song, Y. J.; Fu, H. J.; Jiang, Z. X.; Zhang, X. Z.; Wu, L. N.; Huang, Y. D. *Appl Surf Sci* 2008, 254, 5342.
- Liu, A.; Honma, I.; Ichihara, M.; Zhou, H. *Nanotechnology* 2006, 17, 2845.
- Li, C. Y.; Li, L.; Cai, W.; Kodjie, S. L.; Tenneti, K. K. *Adv Mater* 2005, 17, 1198.
- Li, N.; Li, B.; Yang, G.; Li, C. Y. *Langmuir* 2007, 23, 8522.
- Li, L.; Li, C. Y.; Ni, C.; Rong, L.; Hsiao, B. S. *Polymer* 2007, 48, 3452.
- Zhang, F.; Zhang, H.; Zhang, Z.; Chen, Z.; Xu, Q. *Macromolecules* 2008, 41, 4519.
- Haggenmueller, R.; Fischer, J. E.; Winey, K. I. *Macromolecules* 2006, 39, 2964.
- Coleman, J. N.; Cadek, M.; Blake, R.; Nicolosi, V.; Ryan, K. P.; Belton, C.; Fonseca, A.; Nagy, J. B.; Gun'ko, Y. K.; Blau, W. J. *Adv Funct Mater* 2004, 14, 791.
- Yue, J.; Xu, Q.; Zhang, Z.; Chen, Z. *Macromolecules* 2007, 40, 8821.
- Wang, J.; Khlobystov, A. N.; Wang, W.; Howdle, S. M.; Poliakoff, M. *Chem Commun* 2006, 1670.
- Tran, M. Q.; Shaffer, M. S. P.; Bismarck, A. *Macromol Mater Eng* 2008, 293, 188.
- Du, F.; Fischer, J. E.; Winey, K. I. *J Polym Sci Part B: Polym Phys* 2003, 41, 3333.
- Zhou, C.; Zhuang, Q.; Qian, J.; Li, X.; Han, Z. *Chem Lett* 2008, 37, 254.
- Matsushige, K.; Takemura, T. *J Polym Sci Part B: Polym Phys* 1978, 16, 921.
- Li, J.; Lu, Y.; Meyyappan, M. *IEEE Sens J* 2006, 6, 1047.
- Illers, K. H. *Colloid Polym Sci* 1980, 258, 117.
- Qian, R. *J Macromol Sci Phys* 2001, 40, 1131.
- Nichols, M. E.; Robertson, R. E. *J Polym Sci Part B: Polym Phys* 1994, 32, 573.
- Nichols, M. E.; Robertson, R. E. *J Polym Sci Part B: Polym Phys* 1994, 32, 1607.
- Wunderlich, B. *Crystal Nucleation, Growth, Annealing*; Academic Press: New York, 1976; Vol. 2.
- Kodjie, S. L.; Li, L.; Li, B.; Cai, W.; Li, C. Y.; Keating, M. J. *Macromol Sci Phys* 2006, 45, 231.
- Chang, E. P.; Kirsten, R.; Slagowski, E. *Polym Eng Sci* 1978, 18, 932.
- Park, C.; Lee, K.; Nam, J.; Kim, S. *J Appl Polym Sci* 2000, 78, 576.
- Probst, O.; Moore, E. M.; Resasco, D. E.; Gardy, B. P. *Polymer* 2004, 45, 4437.
- Bhattacharya, A. R.; Sreekumar, T. V.; Liu, T.; Kumar, S.; Ericson, L.; Hauge, R.; Smalley, R. E. *Polymer* 2003, 44, 2373.
- Mago, G.; Fisher, F. T.; Kalyon, D. M. *J Nanosci Nanotechnol* 2009, 9, 3330.
- Zhang, S.; Minus, M. L.; Zhu, L.; Wong, C. P.; Kumar, S. *Polymer* 2008, 49, 1356.
- Garcia-Gutierrez, M. C.; Hernandez, J. J.; Nogales, A.; Panine, P.; Rueda, D. R.; Ezquerro, T. A. *Macromolecules* 2008, 41, 844.
- Yeow, M. L.; Liu, Y. T.; Li, K. *J Appl Polym Sci* 2003, 90, 2150.
- Buonomenna, M. G.; Macchi, P.; Davoli, M.; Drioli, E. *Eur Polym J* 2007, 43, 1557.
- Cheng, L. P.; Lin, D. J.; Shih, C. H.; Dwan, A.; Gryte, C. J. *J Polym Sci Part B: Polym Phys* 1999, 37, 2079.
- Nadkarni, V. M.; Jog, J. P. *Two-Phase Polymer Systems*; Hanser: New York, 1991; Vol. 2, p 213.
- Lin, D.-J.; Chang, C.-L.; Huang, F.-M.; Cheng, L.-P. *Polymer* 2003, 44, 413.
- Mandelkern, L. *Crystallization of Polymers*; McGraw-Hill: New York, 1964.
- Ryan, K. P.; Cadek, M.; Nicolosi, V.; Walker, S.; Ruether, M.; Fonseca, A.; Nagy, J. B.; Blau, W. J.; Coleman, J. N. *Synth Met* 2006, 156, 332.
- Jin, J.; Song, M.; Pan, F. *Thermochim Acta* 2007, 456, 25.
- Mago, G.; Fisher, F. T.; Kalyon, D. M. *Macromolecules* 2008, 41, 8103.
- Kamal, M. R.; Kalyon, D. M.; Dealy, J. *Polym Eng Sci* 1980, 20, 1117.
- Bigg, D. M. *Polym Eng Sci* 1988, 28, 830.
- Sandler, J.; Windle, A. H.; Werner, P.; Altstadt, V.; Es, M. V.; Shaffer, M. S. P. *J Mater Sci* 2003, 38, 2135.
- Khanna, Y. P.; Kumar, R.; Reimschuessel, A. C. *Polym Eng Sci* 1988, 28, 1612.
- Muellerleile, J. T.; Freeman, J. J. *J Appl Polym Sci* 1994, 54, 135.
- Dangseeyun, N.; Supaphol, P.; Nithitanakul, M. *Polym Test* 2004, 23, 187.
- Li, R. K. Y.; Tjong, S. C.; Xie, X. L. *J Polym Sci Part B: Polym Phys* 2000, 38, 403.